Ultramicroscopy 111 (2011) 1581–1591

Contents lists available at SciVerse ScienceDirect

Ultramicroscopy

journal homepage: www.elsevier.com/locate/ultramic

# Introducing measure-by-wire, the systematic use of systems and control theory in transmission electron microscopy

Arturo Tejada [a,*], Arnold J. den Dekker [a], Wouter Van den Broek [b]

[a] Delft Center for Systems and Control, Delft University of Technology, Mekelweg 2, 2628 CD Delft, The Netherlands
[b] EMAT, University of Antwerp, Groenenborgerlaan 171, B-2020 Antwerp, Belgium

ARTICLE INFO

*Article history:*
Received 14 October 2010
Received in revised form
8 May 2011
Accepted 22 August 2011
Available online 7 September 2011

*Keywords:*
High-throughput
Flexible TEM
Systems and control
Defocus control
Thon ring analysis

ABSTRACT

Transmission electron microscopes (TEMs) are the tools of choice for academic and industrial research at the nano-scale. Due to their increasing use for routine, repetitive measurement tasks (e.g., quality control in production lines) there is a clear need for a new generation of high-throughput microscopes designed to autonomously extract *information* from specimens (e.g., particle size distribution, chemical composition, structural information, etc.).

To aid in their development, a new engineering perspective on TEM design, based on principles from systems and control theory, is proposed here: *measure-by-wire* (not to be confused with remote microscopy). Under this perspective, the TEM operator yields the direct control of the microscope's internal processes to a hierarchy of feedback controllers and high-level supervisors. These make use of dynamical models of the main TEM components together with currently available measurement techniques to automate processes such as defocus correction or specimen displacement. Measure-by-wire is discussed in depth, and its methodology is illustrated through a detailed example: the design of a defocus regulator, a type of feedback controller that is akin to existing autofocus procedures.



## 1. Introduction

Transmission electron microscopes (TEMs)[1] are the tools of choice for academic research in material sciences, nanotechnology, and biology. They are also highly valued in, among others, the mining, cement, and semiconductor industries where they are used for production monitoring, control and troubleshooting. In both the academic and industrial sectors, TEMs are increasingly used to perform routine and repetitive measurements in the nano-scale (e.g., counting and measuring nano-particles). Currently, performing such measurements is a labor-intensive task that involves time-consuming steps such as specimen preparation, microscope alignment/calibration and image interpretation. Thus, there is an unequivocal need for a new generation of TEMs capable of self alignment/calibration and of autonomously performing and reporting a range of nano-measurements with *high-throughput*, *following prescribed timing requirements*[2] (as is needed for industrial applications). Rather than image-generating devices, next generation TEMs should be considered measurement tools designed to extract *information* from specimens (e.g., particle size distribution, chemical composition, structural information, etc.) [1]. Clearly, a new engineering perspective is needed to implement this new "specimen-in, information-out" operating philosophy (which is not limited to electron microscopy [2,3]). Such perspective should enable the development of new products in a systematic, *modular* and *flexible* fashion in order to, respectively, reduce the design and development cycle, achieve operation predictability, and enable the low cost expansion of a microscope's capabilities. As will be argued in the following sections, this perspective should be founded on systems and control (S&C) principles, such as model-based control. These are routinely used in many application domains to design automation algorithms that take into account strict throughput and timing conditions, measurement noise, model uncertainties, and perturbations.

Thus, the goal of this paper is to introduce one such perspective called *measure-by-wire* (MBW), which is an extrapolation to electron microscopy of the fly-by-wire concept [4]. Under MBW, an operator is not allowed to directly alter the microscope settings (e.g., he cannot change the microscope alignment). Instead, the operator's role is limited to inserting an appropriate specimen and selecting a desired measurement task, which is then autonomously completed by the microscope. Although the importance of developing autonomous TEMs has been recognized

* Corresponding author. Tel.: +31 15 2781550; fax: +31 15 2786679.
*E-mail addresses:* a.tejadaruiz@tudelft.nl (A. Tejada), a.j.dendekker@tudelft.nl (A.J. den Dekker), wouter.vandenbroek@ua.ac.be (W. Van den Broek).

[1] In this paper the acronym TEM denotes both a microscope (including those capable of scanning) and "transmission electron microscopy".

[2] Note that highly specialized *scanning* electron microscopes that possess some of these features are already available (e.g., CD-SEMs).

0304-3991/$ - see front matter © 2011 Elsevier B.V. All rights reserved.
doi:10.1016/j.ultramic.2011.08.011

before [5], the mechanisms that are proposed here to attain such level of autonomy go beyond the current auto-tuning procedures. The latter are usually separately designed to tune specific parameters in the microscopes (e.g., beam alignment, defocus or astigmatism) and, in general, do not operate concurrently (see [5] and the references therein). In contrast, MBW advocates the use of an integrated hierarchy of local feedback controllers and high-level supervisors (the latter are software programs capable of coordinating multiple components to enforce high-level requirements, such as throughput). This hierarchy should be designed using S&C principles and take into account the interconnections and interdependencies of the main TEM components at the functional level. A global view of these interconnections and interdependencies was developed using currently available information and is presented here, alongside a general set of techniques that could be used to procure missing information. Moreover, a six-steps methodology is proposed to develop the necessary MBW technology. This methodology is illustrated through an example: the design of a defocus regulator (similar but not equal to existing autofocus procedures). This example not only exercises the aforementioned six-steps methodology, but also shows how existing information and measurement techniques can be adapted for feedback control purposes.

The rest of the paper is organized as follows: the current TEM state of the art, from an engineering and high-throughput perspective, is reviewed in Section 2. Section 3 summarizes important S&C concepts and introduces the measure-by-wire concept in depth. It also discusses the benefits and challenges of MBW. Section 4 provides the details of the defocus regulator, including an extension of the diffractogram analysis technique [6] that takes into account (potentially large) variations of defocus during the image acquisition process. Finally, Section 5 contains our conclusions.

## 2. S&C theory as an enabler of autonomous, high-throughput TEM

This section provides an overview of the current TEM automation efforts and their benefits/limitations from the high-throughput operation point of view. It also summarizes the contribution that S&C theory can make towards autonomous, high-throughput TEMs.

### 2.1. The state of the art

As was pointed out, high-tech industries are among the largest current (and future) consumers of TEM technology. Unfortunately, the industrial use of TEMs is nowadays limited by their complex operation, which requires specialized training and is inherently slow. The current manual TEM operation calls for visual inspection of the image quality. When this is lost, an operator must execute multi-step alignment/tuning procedures that involve changing some microscope settings and visually inspecting their effect. Usually, these steps are repeated multiple times before the image quality becomes acceptable again.

During the past 30 years several methods have been developed to automate different aspects of these tuning procedures. As shown in Appendix A, auto-tuning procedures are available to adjust defocus, astigmatism, beam alignment or spherical aberrations in TEMs operating in both scanning and transmission modes. These procedures, except for a few exceptions [7,8], generally combine a *measurement principle* (i.e., a method to estimate a parameter of interest, such as defocus, from images) with a correction mechanism (e.g., changes in the objective lens current). This combination is applied repeatedly until the procedure converges. That is, until a certain qualitative (or quantitative) criterion is met. These algorithms have certainly simplified TEM operation. However, they present some limitations that must be overcome if they are to be used to automate high-throughput TEMs:

- The operator must initiate the auto-tuning procedures and (generally) provide the final assessment of the image quality. Thus, these procedures lack autonomy and cannot automatically correct for changes in the parameters of interest caused by perturbations or noise (e.g., change in defocus due to displacement of the specimen).
- These procedures are not designed to attain high-throughput. The latter is clearly limited in those procedures that use several images to estimate the parameters of interest. However, even those procedures that make use of only one image have limited throughput, since they disregard the transients in the hardware components affected by their correction mechanisms. That is, the necessary images are acquired after the transients in the microscope components have disappeared (e.g., after the specimen holder becomes "stable"). As a consequence, the auto-tuning procedures have an artificial speed upper limit and are (generally) unable to enforce strict timing requirements (e.g., they cannot control their convergence speed).
- Those procedures that converge based on qualitative criteria lack the flexibility required to accommodate changing performance requirements. For instance, an autofocus algorithm based on variance minimization, as in [8], cannot be used to keep the defocus level at a prescribed value (possibly not zero), which may be needed to maximize the precision of a measurement and which may change depending on the specimen (or on the location within a specimen) [1,9].
- Generally, current auto-tuning procedures tune one subsystem at a time, assuming all other subsystems are steady (i.e., do not change) over time. As a consequence, they are difficult to integrate into larger automation schemes that may (possibly) affect multiple related subsystems simultaneously (e.g., displacing the specimen while compensating the defocus).

These difficulties may be overcome by increasing the complexity of the auto-tuning procedures. That is, by increasing the "intelligence" of their accompanying software or by improving their heuristics. This approach, however, may not lead to optimal solutions. Moreover, if it is applied unsystematically it may lead to a collection of ad hoc solutions that have limited portability between different TEM makes and models. A further consequence is that the microscope software becomes more difficult to understand and troubleshoot. What is needed, then, is a systematic approach that helps define clearly the automation objectives, the TEM subsystems that are involved, the measurement techniques that will be used, and how all these are to be integrated. Systems and control theory is such an approach that, as is evident from its long tradition, has been very successful in the automation of complex machines [10–12].

Finally, note that to develop truly autonomous TEMs, new automation algorithms are needed to simultaneously coordinate multiple TEM subsystems. These algorithms should take into account the internal (physical) behavior of individual TEM components, avoiding the common "black box" view. To the best of our knowledge, no such algorithms currently exist. This is due, in part, to the current engineering approach used to design TEMs.

### 2.2. The need for a new engineering perspective

To the best of our understanding, the main hardware components in current TEMs are designed and developed independently by teams of experts, a practice that has yielded highly advanced

and sophisticated TEM components. This practice, unfortunately, has also inhibited the development of a truly holistic TEM design approach from the automation perspective. For example, the specimen holders and the objective lenses are generally designed independently by, perhaps, separate manufacturers. Although their designs obey common electro-mechanical requirements (e.g., size, mechanical tolerances, electronic interfaces, etc.) they do not reflect the *functional dependence*[3] of these components. Thus, although a holder is equipped with local position sensors in all three cartesian coordinates, the sensors' location (in the base of the holder shaft) and precision are such that the sensors cannot be used for defocus correction (which is why the defocus is measured from images and corrected by changing the objective lens current, although it is largely governed by the $z$-position of the specimen).

In general, it seems that although the mechanical and electrical interconnections and interdependencies of the different TEM components are well understood, their functional interdependencies are less so and/or are not taken into account during the design process. Thus, from the functional point of view these components seem to lack modularity and standardized interfaces, which has led to the following difficulties:

- Since TEM components cannot be mixed-and-matched, the maintenance of existing microscopes is a difficult (and expensive) task that requires customized solutions for each individual microscope (i.e., the solution to a problem arising in one microscope cannot be directly ported to another microscope).
- The lack of functional modularity (i.e., clearly defined specifications and limits for the activities of a component or group of components) leads to the so-called "component-entanglement" problem: an observed fault in the microscope cannot be easily traced back to the misbehaving component (or components). This clearly complicates the troubleshooting of faults and has led to the current complex and time-consuming alignment procedures.
- The microscope's functional behavior cannot be easily simulated (there are few models for individual components available), which impedes the rapid testing of new ideas.

Some of these problems can be eliminated (or at least ameliorated) by designing the microscopes with functional integration in mind. Such an approach has been applied successfully to fully automate other micro/nano-scale tools, such as the push-button Phenom scanning electron microscopes (http://www.phenomworld.com) or ASML's wafer steppers (see [12] and references 43 and 44 therein). As mentioned before, this new engineering perspective should be founded on S&C principles for the reasons outlined next.

### 2.3. Benefits of the systems and control approach

The S&C approach relies on two basic concepts (described in Section 3.1): dynamical models and model-based control. These have the following benefits:

- From the S&C viewpoint each component is represented by a dynamical model that describes the component's input–output functionality (see below) and takes into account its transient responses. Developing such models allows one to better understand the functional interactions and interdependencies among components and to choose a suitable control (i.e., automation) strategy. Thus, in general, components with no functional interdependencies are controlled using single-input–single-output control techniques [13], while a group of functionally dependent components can be controlled via multiple-input–multiple-output techniques [14]. Moreover, from the S&C perspective two (groups of) components with similar input–output functionality are indistinguishable from each other. Thus, the use of dynamical models also fosters component modularity and the portability of automation solutions.
- Automation schemes based on model-based control (see below) are systematic and, by definition, avoid the component-entanglement problem. Model-based controllers are capable of enforcing strict timing requirements, reject perturbations and noise, and take into account modeling deficiencies. Moreover, they can also be equipped with online adaptation capabilities to account for changes in the components (e.g., wear and tear, actuator faults, etc.) or in the microscope's performance requirements.

An approach that reflects these ideas follows.

## 3. A new TEM paradigm: measure-by-wire

As mentioned before, measure-by-wire is implemented using concepts from systems and control theory. Thus, some of these are summarized first.

### 3.1. Systems and control concepts

*System*: It is a device that transforms input signal(s) (e.g., voltages or currents) into output signal(s) (e.g., focal distance, astigmatism, position, etc.). As shown in Fig. 1, inputs and outputs are denoted, respectively, $u(t)$ and $y(t)$ ($t$ denotes time). Examples of systems in a TEM are the objective lens (input: current; output: focal distance), the beam deflectors (input: currents; output: beam displacement), and the specimen holder (inputs: voltages; output: specimen position).

*Dynamics*: This refers to an important system property: transient behavior (or memory). A system presents transient behavior when an expected change on its output, due to a specific change in its input, is not instantaneous (see Fig. 1a). For example, the specimen holder possesses dynamics since a step change in its input voltage produces a step change in the sample position only after some delay. The input–output dynamics of a system are usually described by a *dynamical model* [13].

*Model-based control*: It is the use of feedback and/or a feedforward controllers (see Fig. 1b) to force the output of a system to behave as desired (e.g., force a lens to reach a new focal distance within 1 s from a change on its input current). The controllers are designed based on the system's dynamical model and are used to modify the system input based on measurements of the system output (from a sensor) and/or on a reference input.

*Image-based control*: It is the particular instance of model-based control where the sensor is image-based. In this case, the controller is designed taking also into account the dynamics of the image formation process and those of the image processing algorithm that produces the sensor's output. Image-based control is indispensable to control systems with outputs such as defocus or specimen drift, which cannot be measured directly through standard sensors.

*Controller auto-tuning*: This is an advanced S&C technique that allows a feedback (or a feedforward) controller to modify its own structure "on-the-fly" in response to detected changes in the system it controls. That is, the controller adapts to changing operating conditions.

[3] Here, "functional dependence" denotes the activities of one component that may influence (or interfere with) the activities of another.

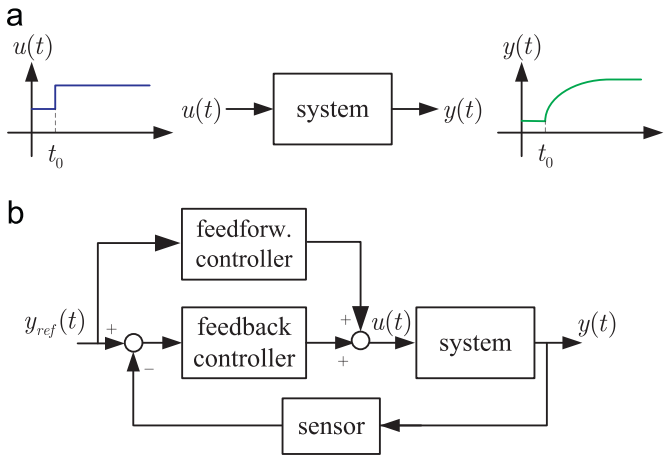


**Fig. 1.** (a) An example of a system and its transient behavior. (b) General setup of model-based control, including feedback and feedforward controllers. $y_{ref}(t)$, $u(t)$ and $y(t)$ represent, respectively, the reference signal, the system input and the system output.

### 3.2. The measure-by-wire concept

MBW parallels fly-by-wire in modern aircraft. In such aircraft, the pilot has no direct control of the aircraft's control surface actuators (e.g., the engines, ailerons or rudder). Instead, his role is limited to providing high-level commands, such as "turn the aircraft 180°" or "follow flight path x", to the onboard computer. These commands are then autonomously executed by the computer, which generates and coordinates the appropriate sequence of orders for the actuators, based on flight data from multiple sensors (e.g., attitude, wind speed, etc.) [4]. That is, the aircraft is operated *without a human in the loop*.

MBW extends this approach to transmission electron microscopy. Specifically, in a measure-by-wire TEM the operator has no direct control (neither mechanically nor electronically) of internal components such as the specimen holder or the objective lens. His role is limited to loading the specimen to be analyzed and selecting the desired measurement tasks. The microscope's computer then automatically identifies the actions needed to perform the measurements (e.g., sample translation, change of magnification, change of defocus, etc.), issues appropriate orders to the necessary components, and acquires and processes the sensor data (e.g. images or signals) necessary to render the measurements. Clearly, a measure-by-wire TEM operates *without an operator in the loop*.

The following steps are proposed to develop the technology necessary for MBW:

1. Determine the allowed range of specimens types (e.g., crystals, particles on amorphus substrates, etc.). Define the range of measurement tasks that the microscope should be able to perform.
2. Determine the microscope operating conditions that correspond to the measurement tasks and specimen types described in step 1. Operating conditions of interest include the value ranges for defocus, astigmatism, coma, sample-drift rate, lenses' input currents, etc. They also include the image types and imaging modes.
3. For relevant TEM components, determine the relevant input and output signals and develop (or reuse) methods to measure them (i.e., sensors). Note that many of these signals can be measured directly (e.g., currents). However, some must be measured through indirect methods (e.g., sample drift).
4. Derive dynamical models for these components. The models should relate the input and output signals of interest and be valid under the determined operating conditions.
5. Develop (local) controllers for each component or group of related components, using techniques (e.g., robust control [15]) that can cope both with the perturbations present in the microscope (e.g., specimen drift) and with model uncertainties. These controllers should also meet performance requirements compatible with the measurement tasks defined in step 1.
6. Develop high-level supervisors capable of coordinating multiple components to execute high-level commands. Such supervisors could be developed through techniques for the control of discrete-event systems (see e.g., [16]). The high-level supervisors could also provide auto-tuning capabilities to the local controllers.

It follows from this methodology that MBW presents multiple benefits. Among them:

*Increased performance*: Since the operator's control of internal TEM components is restricted, the microscopes can be operated at internal regimes that may not be compatible with human use. For instance, control actions could be generated in between image acquisitions and during component transients in order to speed up the response of some components. Moreover, images could be acquired even while the specimen holder is moving, provided that the motion is recorded for subsequent image de-blurring. Additionally, the control system could compensate for perturbations faster than the operator. In all these cases, the measurement throughput and accuracy would be increased.

*Reduced complexity*: The operator interfaces (e.g., joysticks, phosphorous screen, aperture selectors, etc.) would be removed. Moreover, the use of appropriate models and robust control techniques would also allow for components with greater manufacture tolerances and, potentially, lower manufacturing costs.

*Carefree operation*: The operator's inputs would be automatically restricted when they exceed the microscope's operating limits (e.g., the operator would not be allowed to de-align the TEM column).

*Cost reduction through modularity & standardization*: This is a direct benefit of the S&C approach (see Section 2.3), which drives down development costs and facilitates new product development.

*New TEM simulation tools*: Based on the collected dynamical models and the integration model described below, it will be possible to develop a detailed TEM functional simulation. Such simulation platform would in turn serve as a test bed for new prototype microscopes.

On the other hand, MBW also offers significant challenges:

*Image-based sensors for control*: There are currently no sensors capable of *directly* measuring variables such as defocus, astigmatism, or specimen position. Nevertheless, controlling these variables is necessary for TEM automation. These variables are currently estimated from images through algorithms that are sensitive to the specimen type and/or limited in their speed (see Table A1 and [17]). This has significant implications for control development. For instance, the dependence on the specimen type impedes the continuous application of feedback (the portion of the specimen under inspection may not always be suitable for estimation purposes), while the slow estimation speed (up to several seconds) requires the use of special control techniques capable of handling large sensor delays. Thus, to enable MBW new direct-measurement sensors or better estimation procedures must be developed. However, as is shown in Section 4, current estimation procedures can be adapted for control purposes.

*Dynamical models*: These models must be derived either from physical principles or through identification experiments. The latter are usually unavoidable due to the complex physical processes in many TEM components. Fig. 2a shows the basic experimental setup needed to identify the model of a generic TEM

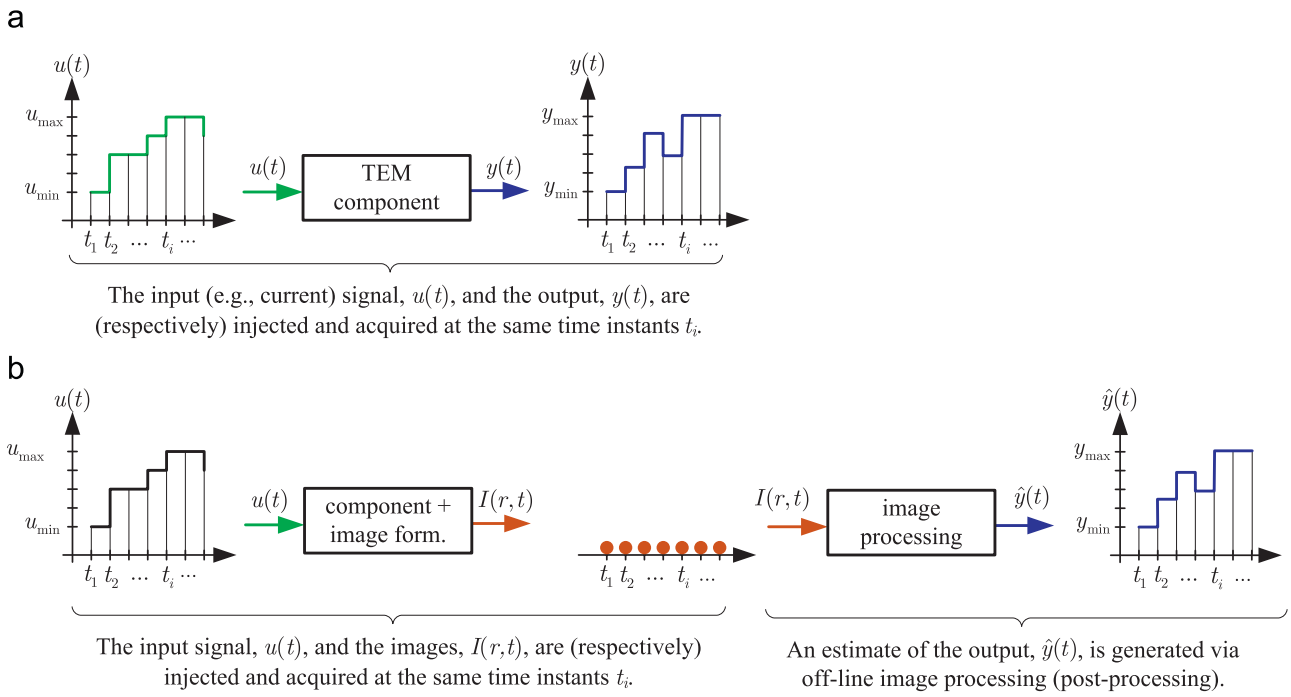


**Fig. 2.** Setup of the model identification experiments for a generic TEM component. (a) The component's output, $y(t)$, is directly measurable by a sensor. (b) The component's output must be estimated from images. $r$ and $t$ denote, respectively, spatial and time coordinates.

component. The experiments consists of physically injecting a signal $u(t)$ (a voltage or current) in the component's input and simultaneously measuring the component's output, $y(t)$. From this input–output data a model can be built using well-known techniques [18,19]. If, as is often the case, $y(t)$ can only be estimated from an image (e.g., astigmatism), then the model is built using an estimate, $\hat{y}(t)$, derived from the images, $I(r,t)$, via a suitable image processing program. As is shown in Fig. 2b for identification purposes the image processing can be done off-line. Note, however, that the resulting model will not only describe the dynamics of the TEM component under consideration, but also those of the image formation process. Also note that the faster the images are acquired (e.g., 20 images per second) the more descriptive the resulting model would be (such image rates could be reached using stroboscopic techniques, see [20] an the references therein). Finally, note that for control purposes the dynamics of the image processing program become relevant and must themselves be characterized.

Setting up and performing identification experiments is a challenging task. Nevertheless, it is a *necessary* task, since dynamical models of several components (e.g., the objective lens, the beam deflectors, etc.) are needed to develop high-throughput microscopes. To see this, consider the following scenario:

> Suppose that the size distribution of spherical particles that lie in a specimen of area 0.1 mm $\times$0.1 mm and have a known average diameter of 10 nm must be estimated from TEM images. Let the image size be 512 $\times$512 pixels, the pixel size be 2 nm $\times$2 nm (i.e., 5 pixels per particle diameter), and the image integration time be 0.6 s. Finally, assume that a (modest) throughput of two processed specimens per hour is to be attained.

Under the stated conditions, nearly 10,000 images are needed to measure *all* the particles in each specimen. However, using statistical methods the number of images needed could be reduced to, for instance, 500 per specimen. This in turn implies that at least one payload image (i.e., an image from which the particles can be measured) must be taken every 3.6 s. Since the specimen position and, possibly, the defocus must be adjusted between payload image acquisitions, both the specimen holder and the objective lens should be able to react in less than 1.5 s (assuming they do not operate concurrently). Even less time would be available if the camera readout time, bigger specimens, smaller particles, or higher throughput are considered. Clearly, then, the transient response of the holder, the lens, and other components must be characterized and well understood.

*Integration model*: It is clear that to enable automation and model identification a new integrative engineering perspective must be developed. Such perspective should take into account the input–output behavior of each component and the components' interactions and interdependencies. Moreover, since different component settings yield different kinds of images (e.g., diffraction patterns, bright field images, etc.) that, in turn, contain different information, any integration model should emphasize the influence of each component in the image formation process.

The next subsection describes one such model from the vantage point of systems and control.

### 3.3. Control-oriented integration model

The proposed integration model is shown in Fig. 3. It classifies the TEM components into three groups: optics, mechanics, and sensor. This model loosely follows the component classification into illumination system, objective lens/stage, and imaging system proposed in [25]. Note, however, that this model is an abstraction intended for analysis and automation purposes and may not completely coincide with the physical makeup of a given microscope.

*The optics*: This group contains the components that set the microscope's optical properties: the objective lens, the beam deflectors, the electron gun, etc. Each component takes a current (or voltage) as input and generates an optical parameter as output. For example, the objective lens maps a current into the focal distance, $f(t)$, and the beam deflectors transform voltages into the beam displacement, $r_d(t)$. Note that the inputs of these

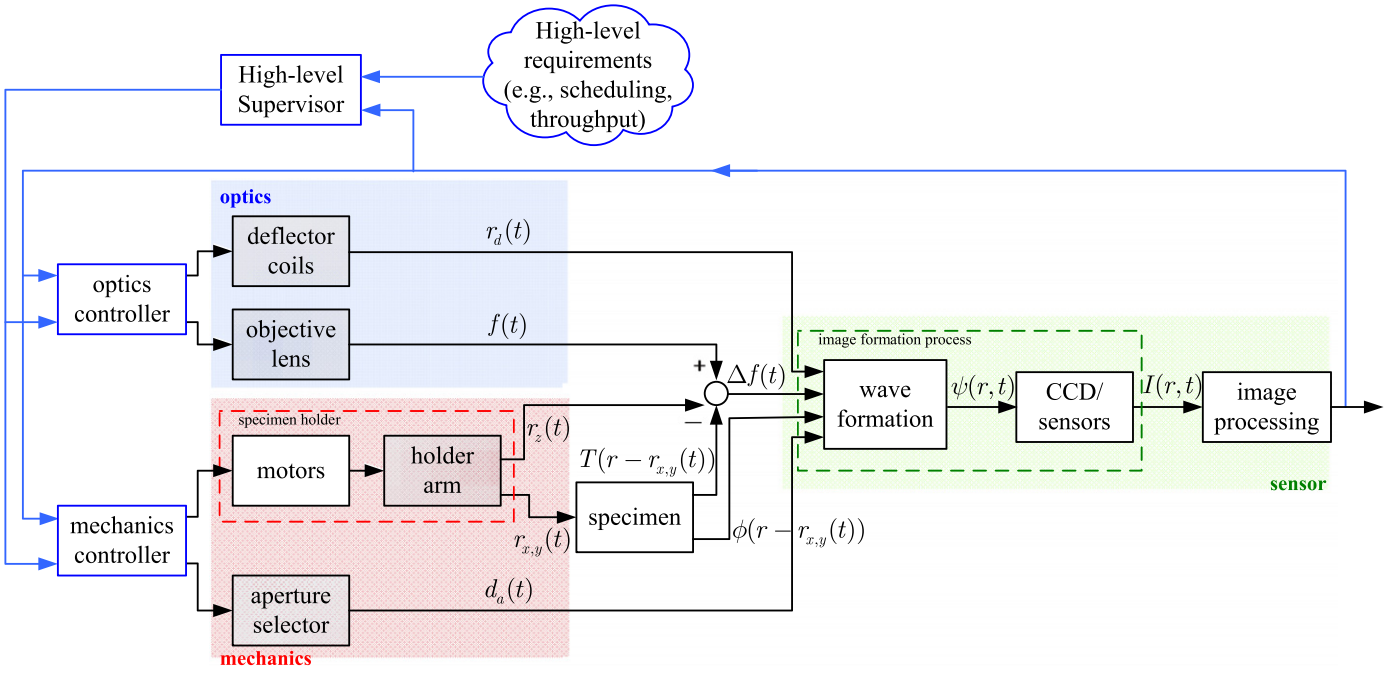


**Fig. 3.** Control-oriented integration model.

**Table 1**
Available information on TEM component dynamics and their control.

| Group | Available models | Current controls |
|---|---|---|
| Optics | Static input–output models for most optical components are known to exist. They form part of the intellectual property of TEM manufacturers and are used in all computer-controlled TEMs to adjust the defocus and other parameters. Although there has been a recent effort to characterize the dynamics of an objective lens [21], complete input–output dynamical models for such lenses are not readily available. | The inputs to these components are locally controlled. However, their outputs are currently *not* regulated through feedback control (i.e., the optics controller is currently not implemented). |
| Mechanics | Dynamical models are available for the motors in the specimen holder [22]. However, models relating the motor inputs to the current specimen position are not available (the effect of the specimen holder's arm is unknown). Models for the aperture selector motors are not available. | The angular positions of the motors in the specimen holder are currently controlled through a feedback PID compensator. However, the specimen's position is currently *not* controlled through the mechanics controller. No information is currently available about the aperture selector control. |
| Sensor | Detailed static models for the image formation process, the CCD camera and the estimation algorithms are available in the literature (see, e.g., [23,24] and Table A1). | |

subsystems are locally controlled through current or voltage regulators (not shown in Fig. 3).

*The mechanics*: This group includes the specimen holder and the aperture selector (which is motor controlled). The specimen holder is directly responsible for the specimen's $x$–$y$ position, $r_{x,y}(t)$, vertical position, $r_z(t)$, and tilting angles $\alpha(t)$ and $\beta(t)$ (not shown in Fig. 3). Indirectly, it also determines the objective lens defocus, $\Delta f(t)$, since $\Delta f(t)=f(t)-(T(r-r_{x,y}(t))+r_z(t))$, where $r$ denotes $x$–$y$ position, and $T(r)$ describes the apparent vertical displacement of the specimen due to changes in its topology. The aperture selector is responsible for choosing the size, $d_a(t)$, and location of the apertures in the column (e.g., the objective aperture), which in turn influence the resulting image type.

*The sensor*: This group incorporates the components and processes that generate the images. This includes the image formation process (which determines the mathematical model of the acquired images, $I(r,t)$), the CCD detector (or the BF, ADF, or HAADF sensors), and the image processing algorithms.

Fig. 3 makes clear the functional interdependencies among the TEM components. It also helps to make clear the currently available information for control purposes. This information is summarized in Table 1 and is the basis for the research described next.

## 4. Defocus regulation

The defocus regulation problem was introduced in [17]. The objective of defocus regulation is to force the objective lens defocus, $\Delta f(t)$, to be as close as possible to a prescribed defocus reference value, $\Delta f_{ref}$, no later than $\tau$ seconds after the reference value is set ($\tau$ is a prescribed constant). This requires one to develop an objective lens controller capable of enforcing the condition

$$|\Delta f(t)-\Delta f_{ref}|<\varepsilon \tag{1}$$

for a prescribed error bound $\varepsilon>0$ and for all $t>\tau$ (assuming $\Delta f_{ref}$ is set at $t=0$). Defocus regulation was chosen for several reasons: (i) it demonstrates the MBW methodology, (ii) it is conceptually simple from a control viewpoint, (iii) it shows how existing estimation methods (for optical aberrations) could be used (or extended) for control purposes, and (iv) it is indispensable for TEM automation (to compensate for defocus perturbations).

Defocus regulation exercises steps 1–5 in the MBW methodology. Specifically:

1. The operator sets the desired values for $\Delta f_{ref}$ and $\varepsilon$ and provides a specimen with large amorphous backgrounds.

2. The microscope operates under the following conditions: the electron beam and the specimen holder are stationary; the specimen is flat and located at the eucentric plane, $Z_{ref}$, and its thickness is less than 20 nm (so the weak phase object approximation applies); the defocus range is 1–10 Scherzers; all optical aberrations have been canceled (except, of course, the spherical aberration); and the magnification and the apertures are fixed to maximize the images' spatial frequency information. Under these conditions, the integration model is simplified to the feedback loop in Fig. 4 (see also [17, Fig. 3]). Only bright field images, in transmission mode, are considered. These, based on the above assumptions, are described mathematically as follows [23]:

$$I(r,t) = |\phi(r) * h(r,t)|^2, \tag{2}$$

where $r=(x,y)$ denotes position in the image plane; $\phi(r) \triangleq \exp(j\varsigma V_p(r))$ is the specimen's transmittance function (based on the phase object approximation), $j=\sqrt{-1}$, $\varsigma$ is the interaction constant, $V_p(r)$ is the specimen's projected potential function; and $*$ denotes the convolution operator over $r$. Furthermore,

$$h(r,t) = \mathfrak{F}^{-1}\{H(q,t)\},$$

$$H(q,t) \triangleq A(q)E(q)\exp(j\chi(q,t)),$$

where $\mathfrak{F}$ denotes the Fourier transform over $r$, $q=(u,v)$ denotes position in the spatial frequency plane, $A(q)$ is the aperture function, $E(q)$ is the temporal coherence envelope function (no spatial incoherence is assumed), and

$$\chi(q,t) = \pi(0.5C_s\lambda^3|q|^4 - \Delta f(t)\lambda|q|^2) \tag{3}$$

($C_s$ is the coefficient of spherical aberration and $\lambda$ is the electron wavelength). Moreover, since the specimen in very thin (by assumption), (2) can be approximated as follows [26]:

$$I(r,t) \approx 1 + 2\varsigma V_p(r) * \mathfrak{F}^{-1}\{A(q)E(q)\sin(\chi(q,t))\}. \tag{4}$$

Finally, the images are acquired with a CCD camera with an integration period, $T$, of 100 ms.

3. The component of interest is the objective lens. As a system, this lens has a single input, $u(t)$ (electrical current), and single output, $\Delta f(t)$ (defocus), which should be measured for control purposes. Defocus is usually estimated by fitting $H(q,t)$ (or a function derived from it) to the Fourier transform of a bright field image of an amorphous material [6,27–29]. These methods usually assume that the defocus is constant while the image is acquired. That is, the images used to estimate the defocus are acquired only when the defocus is stable. This practice, however, limits the speed at which the defocus can be stabilized. In such case, it can be shown that the image produced a TEM's CCD camera, $I_{bf}$, is proportional to a time integral of the image model in (2) (see the companion paper [30] in this issue for details). That is,

$$I_{bf} \propto \int_{t_o}^{t_o+T} I(r,t)\,dt,$$

where $\propto$ indicates $I_{bf}$ is proportional to the right-hand-side integral. Under the conditions leading to (4) the above integral can be computed as

$$\int_{t_o}^{t_o+T} I(r,t)\,dt \approx T + 2\varsigma V_p(r) * \mathfrak{F}^{-1}\left\{A(q)E(q)\int_{t_o}^{t_o+T}\sin(\chi(q,t))\,dt\right\}.$$

Furthermore, if the defocus variation can be (approximately) assumed to be linear with time, that is, if $\Delta f(t) \approx \Delta f(t_o) + m_{t_o} t$, $t \in [t_o, t_o+T)$, then it follows from (3) that

$$\int_{t_o}^{t_o+T} I(r,t)\,dt \approx T + 2\varsigma V_p(r) * \mathfrak{F}^{-1}\{A(q)E(q)E_{t_o}(q)\sin(\tilde{\chi}(q))\}, \tag{5}$$

where

$$E_{t_o}(q) \triangleq \operatorname{sinc}\left(\frac{\pi\lambda|q|^2 m_{t_o} T}{2}\right)$$

and

$$\tilde{\chi}(q) \triangleq \pi\left(0.5C_s\lambda^3|q|^4 - \lambda|q|^2\left(\Delta f(t_o) + \frac{m_{t_o}T}{2}\right)\right).$$

Note that (5) reduces to (4) when the defocus is constant. Moreover, (5) indicates that the defocus of bright field images acquired under the conditions that make it valid (i.e., thin specimen and approximately linear defocus variation) can be estimated using modified versions of the estimators in [6,27–29] (such estimators should take into account the extra envelope function $E_{t_o}(q)$). As is shown in [17] the output of such estimators, $\Delta\hat{f}(t)$, would be of the form

$$\Delta\hat{f}(t) = a\Delta f(nT) + b,$$

$t \in [nT,(n+1)T)$, $n=0,1,\ldots$, where $a$ and $b$ are constants that must be obtained experimentally or through simulations.

4. There are currently no dynamical models available in the literature that relate the input current, $u(t)$, of a TEM objective lens with its focal distance, $f(t)$. To the best of our knowledge, the closest related work is [21], which reports the steps taken towards developing such a model in a scanning electron microscope.

A lens' input–output relationship is difficult to model precisely. However, as a first approximation, it can be assumed that there is a static (but perhaps nonlinear) relationship between the magnetic field inside the lens and its focal distance [23]. The magnetic field, in turn, is set by the current in the lens coil, which is governed by the lens electronics. Moreover, most coils present some level of electrical resistance, capacitance and self-inductance. Thus, it is reasonable to assume that the lens

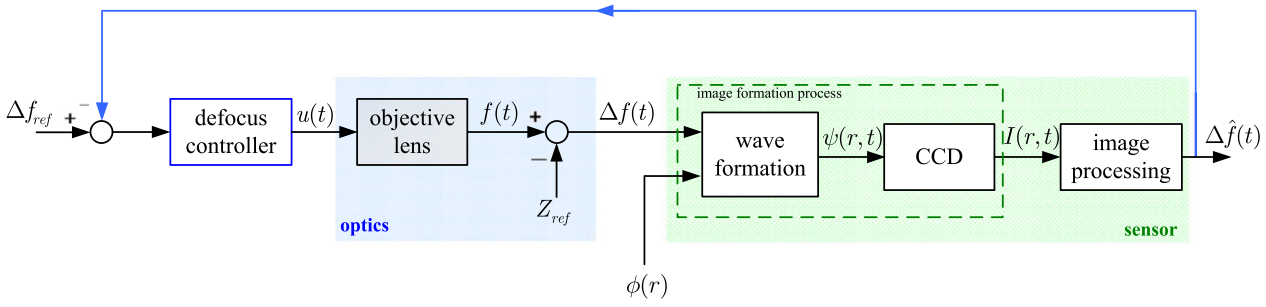


**Fig. 4.** Defocus regulation feedback loop.

electronics behave as a resistor–inductor–capacitor circuit (cf. [31] for an alternative viewpoint). It follows from this assumption that the dynamics of the lens can be described by a second-order ordinary differential equation. Thus, recalling that $\Delta f(t) = f(t) - Z_{ref}$ (see Fig. 4) one can write without loss of generality [13]

$$\frac{d^2\Delta f(t)}{dt^2} + 2\xi\omega\frac{d\Delta f(t)}{dt} + \omega^2 = \kappa\omega^2 u(t), \tag{6}$$

where $\xi$, $\omega > 0$, and $\kappa \in \mathbb{R}$ (respectively, the damping coefficient, the natural oscillation frequency, and the steady-state gain [13]) are parameters that must be determined experimentally, since they depend on the physical characteristics of the particular objective lens under consideration.

To determine these parameters and to validate model (6), identification experiments (see Section 3.2) were performed in a FEI Tecnai F-20 (equipped with a TWIN objective lens) and in a Jeol JEM-3000F.[4] For each experiment, the microscope settings were adjusted to match the conditions given in step 2 (see above). Each experiment consisted of two step tests performed in succession. The tests comprised the following steps: (a) the defocus was set to an initial underfocus value, $\Delta f_{ini}$ (i.e., the input current value was set to $u(t) = \Delta f_{ini}/\kappa$); (b) bright field images of an amorphous specimen were acquired at a constant image rate for $T_{step}$ seconds; (c) at that time, without stopping the image acquisition, a step change in the defocus level was performed by adding $\Delta f_{step}$ to it (i.e., $u(t)$ was set to $(\Delta f_{ini} + \Delta f_{step})/\kappa$); (d) after a few additional seconds the image acquisition was stopped. Note that all changes to the defocus level were done by software (i.e., $u(t)$ was not directly measured and no additional hardware components were connected to the lens). Also note that $\Delta f_{ini}$ and $T_{step}$ were not measured directly. Instead, they were estimated from the data (see Appendix B). For comparison purposes, $\Delta f_{step}$ was also estimated from the data. The nominal values of the microscope settings are given in Table 2, and the experimental results are shown in Figs. 5 and 6.[5] The results suggest that the transients in the Tecnai's lens (i.e., the time it takes the lens to reach $\Delta f_{ini} + \Delta f_{step}$ once the defocus step is commanded) last between 0.3 s and 0.4 s (defocus values between $\Delta f_{ini}$ and $\Delta f_{ini} + \Delta f_{step}$ are visible in three or four images after $T_{step}$). Similarly, the transients in the JEM seem to last between 1.13 s and 1.7 s. Also note that in the second experiment $\Delta f_{ini}$ varied slightly from test 1 to test 2, although the same initial current was used for each test. This may suggest the presence of hysteresis in the lens. Although model (6) does not take hysteresis into account, it can still mimic the observed lens behavior if one takes

$$u(t) = \begin{cases} \Delta f_{ini}/\kappa, & t < T_{step}, \\ (\Delta f_{ini} + \Delta f_{step})/\kappa, & t \geq T_{step}. \end{cases} \tag{7}$$

Fitting the known response of model (6) to the input signal $u(t)$ in (7) to the recorded data using the minimum square error approach (see Appendix B), it was found that model (6) fits the Tecnai's experimental data best when $\xi = 1.13$ and $\omega = 24.82$ ($\kappa$ was not estimated because the lens' input current was not recorded). This can be seen in Fig. 5, which shows in solid lines the results obtained after simulating model (6) with Matlab [32] (for this simulation, $\kappa$ was set to 1). Similarly, model (6) with $\xi = 0.76$ and $\omega = 3.04$ fits the JEM's experimental data with minimum square error.

[4] Technical details about these microscopes can be found at the manufacturer's websites: www.fei.com and www.jeol.com.

[5] We thank Dr. Seyno Sluyterman (FEI Company) for his support in collecting this data, which is available at http://www.tejadaruiz.net/files/UM2011data.zip.

**Table 2**
Nominal values of the microscope settings used in the identification experiments.

| Settings | Tecnai F-20 | JEM 3000F |
|---|---|---|
| $\lvert\Delta f_{step}\rvert$ (nm) | 250 | 450 |
| Images per second | 10 | 1.76 |
| Integ. time (ms) | 100 | 100 |
| Image size (pixels) | 668 × 668 | 256 × 256 |
| Pixel size (nm$^2$) | $0.096^2$ | $0.0837^2$ |
| $C_s$ (mm) | 1.01 | 1.3 |
| Gun voltage (kV) | 201 | 300 |
| Amorphous specimen | Carbon | Carbon |

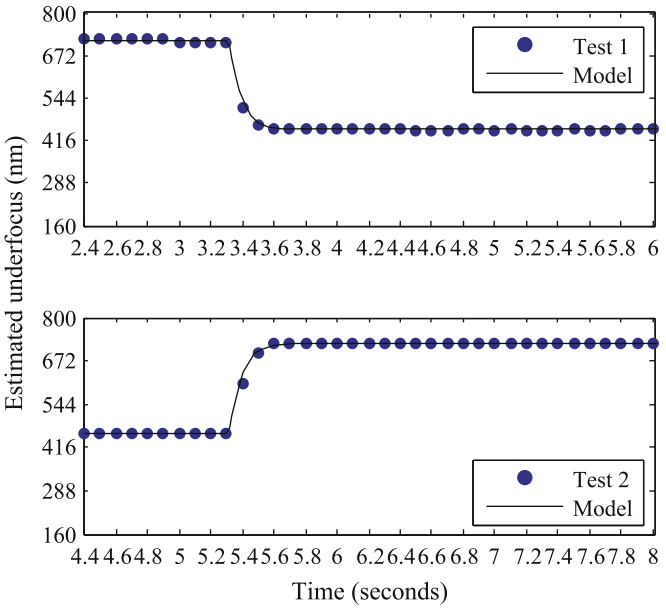


**Fig. 5.** Tecnai F-20's identification experiment results (variation of the objective lens defocus over time in response to a step change in the lens input current). Estimated parameter values: $\Delta f_{ini} = 717$ nm, $\Delta f_{step} = -268$ nm, $T_{step} = 3.3$ s (Test 1); $\Delta f_{ini} = 458$ nm, $\Delta f_{step} = 263$ nm, $T_{step} = 5.3$ s (Test 2). The simulated behavior of model (6) with $\xi = 1.13$ and $\omega = 24.82$ (for both tests) is shown in solid black lines.

Clearly, only a limited amount of step tests were performed. Thus, it is not possible to quantify the error in the estimation of $\xi$ and $\omega$, nor to qualify the generality of model (6). Also, note that (6) could be extended to include hysteresis, for which controller design methods are available [33]. Nevertheless, as it is, this preliminary model provides enough information to illustrate the benefits of the model-based control approach, as is discussed next.

5. As mentioned in Section 3.1, the role of the controller is to shape the input of a system so its output exhibits a prescribed behavior (see Fig. 1). A controller is typically a real-time computer program that computes and injects (via a digital-to-analog converter) a new input value at regular intervals, $T_s$, which are shorter than the system's time constants. A feedback controller performs this calculation based on the difference, $e(t)$, between the desired output value, $y_{ref}$, and the *measured* output value, $y(t)$, and on one of the several control algorithm available in the literature (e.g., PID control, $\mathcal{H}_\infty$ control, etc. [15]). The control algorithm is selected based on the properties of the system and on the desired properties of the output. The latter includes, for example, allowed errors, immunity to perturbations, etc.

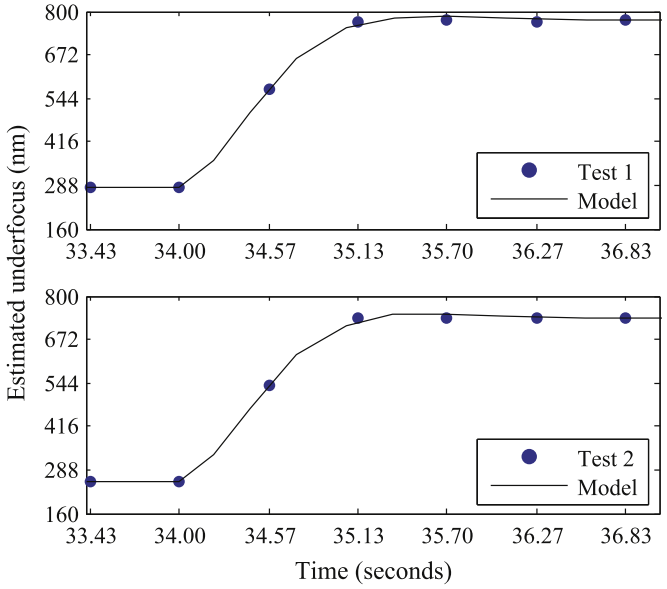


**Fig. 6.** JEM 3000F's identification experiment results (variation of the objective lens defocus over time in response to a step change in the lens input current). Estimated parameter values: $\Delta f_{ini}=283$ nm, $\Delta f_{step}=489$ nm, $T_{step}=34$ s (Test 1); $\Delta f_{ini}=252$ nm, $\Delta f_{step}=483$ nm, $T_{step}=34$ s (Test 2). The simulated behavior of model (6) with $\xi=0.76$ and $\omega=3.04$ (for both tests) is shown in solid black lines.

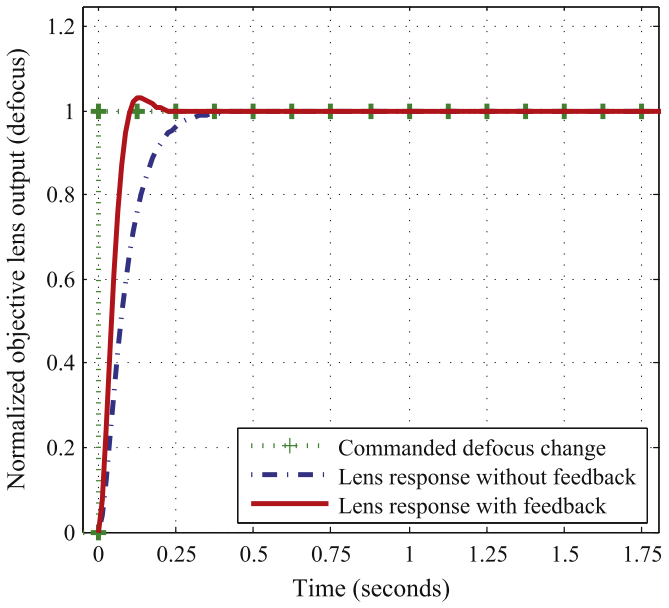


**Fig. 7.** Normalized simulated response of an objective lens to a commanded step change in defocus ($T_{step}=0$), using the Tecnai lens model (that is, model (6) with $\xi=1.13$, $\omega=24.82$, and $\kappa=1$).

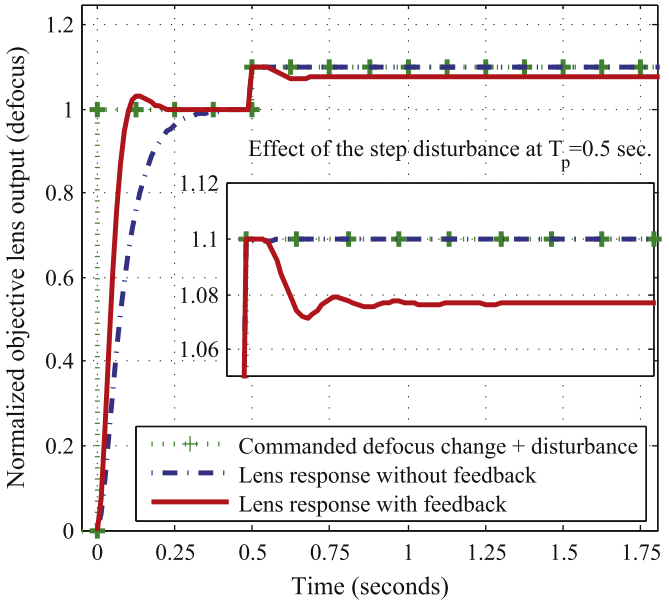


**Fig. 8.** Effect of a 10% step disturbance in the specimen vertical position, $Z_{ref}$. The perturbation is injected at time $T_p=0.5$ s.

Thus, consider again the defocus regulation problem (1). Suppose that $\Delta f(t)=\Delta f_{ini}$ for $t<T_{step}$ and that at time $t=T_{step}$ the operator sets a new desired defocus value, $\Delta f_{ref}=\Delta f_{ini}+\Delta f_{step}$. Then, the defocus regulation problem states that the defocus should reach (and stay within) the value range $(\Delta f_{ref}-\varepsilon,\Delta f_{ref}+\varepsilon)$ in no more than $\tau$ seconds.

Now, if the lens dynamics are linear, as it is suggested by model (6), it can be shown that the time it takes the defocus to reach $(\Delta f_{ref}-\varepsilon,\Delta f_{ref}+\varepsilon)$ is independent of $\Delta f_{step}$, provided that $\varepsilon$ is proportional to $\Delta f_{step}$. Thus, without loss of generality, it will be assumed that $\Delta f_{ini}=T_{step}=0$, $\varepsilon=0.01\Delta f_{step}$.

The Tecnai lens response to a commanded step change in defocus was simulated under these conditions, and the normalized response (i.e., $\Delta f(t)$ divided by $\Delta f_{step}$) is shown in Fig. 7. This figure shows that the lens output takes about 0.33 s to reach the range (0.99,1.01). Thus, without feedback control, the lens satisfies the defocus regulation problem for $\tau\geq 0.33$ s. Although it is tempting to conclude that, based on this model, the lens can be operated quickly and accurately without feedback control, in practice model (6) is not valid for all possible values of the input current $u(t)$ (e.g., the lens hysteresis could be stronger for larger input currents). Moreover, by itself the lens cannot correct for perturbations in the defocus level. The latter are known to happen when, for instance, the specimen is laterally displaced and are, perhaps, one of the main reasons why the defocus must be regularly adjusted in current TEM. Finally, note that current autofocus algorithms based solely on image analysis can only correct the defocus *after* one or more images have been acquired. If the images are acquired after the transients have subsided, then an autofocus algorithm that makes use of $n$ images would require at least $0.33n$ seconds to adjust the defocus (assuming that the image processing time is negligible). Clearly, this is not compatible with high-throughput scenarios (this is specially true for the JEM 3000F, since its lens has a transient time of over 1 s).

In contrast, the use of a feedback controller can help to reduce the impact of perturbations and model uncertainties, and can also speed up the lens response time. The latter is possible because a controller can change the lens current even *during* an image acquisition. To do so, the controller makes use of the model prediction principle. That is, it runs an internal "simulation" of the lens dynamical model to "predict" the value of lens output, $\Delta f(t)$, while the image is being acquired. The error signal, $e(t)=\Delta f_{ref}-\Delta f(t)$, is then estimated from this prediction and used to compute the control action $u(t)$. This procedure is repeated until the image acquisition is completed and the image has been processed. The measured defocus value, $\Delta\hat{f}(t)$ (see Fig. 4), is then used to correct the controller's internal simulation (to minimize the prediction error) and the whole procedure is repeated.

Fig. 7 shows the simulated Tecnai lens response to a commanded step change in defocus when it is equipped with

a feedback controller that uses a "predictive observer" (the simplest application of the prediction principle [34]) and a proportional control algorithm (i.e., the controller acts as static multiplier with unitary gain, so $u(t)=e(t)$), with $T_s=12.5$ ms. Clearly, the feedback controller speeds up the lens response (it now satisfies the defocus regulation problem for $\tau \geq 0.19$). Moreover, as shown in Fig. 8, this simple feedback controller also helps to ameliorate the impact of perturbations, although it was *not* specifically designed to do so. In this figure, a step perturbation of magnitude $0.1\Delta f_{step}$ has been injected to the specimen's vertical position. Without feedback control this perturbation is directly translated into a 10% increase of defocus. However, using the feedback controller the defocus increase is reduced to 7.9% (approximately). This can be further reduced by designing the controller (using specialized control algorithms such as $\mathcal{H}_\infty$ [15]) to both speed up the lens response and reject perturbations (without oscillations).

## 5. Conclusions

TEMs are the tools of choice for academic and industrial research in the nano-scale. As a consequence, there is a clear need for a new generation of autonomous (operator-free), high-throughput, TEMs that operate under the "specimen-in, information-out" philosophy. To aid in their development, measure-by-wire (MBW) was proposed as a new engineering perspective for TEM development. Under this perspective, a microscope operator would yield the control of the microscope's internal processes to a hierarchy of feedback controllers and high-level supervisors who, in turn, directs the microscope operation.

High-throughput automation relies on a clear understanding of the dynamical properties of the main TEM components. This understanding is, in turn, translated into a set of dynamical models that lie at the center of the control design. Although dynamical models are not currently available for many TEM components, it was shown that they could be developed from available information and from data collected from well-designed model identification experiments.

A detailed example of the MBW approach was provided through the development of an objective lens dynamical model and a defocus regulator. This example includes an extension of the classical Thon rings fitting technique that incorporates the effects of time varying defocus during the image formation process. Moreover, it was shown that the defocus regulator can increase the reaction speed of the lens and its resilience to perturbations.

Research is on its way to improve the objective lens model, the defocus measurement speed, and the properties of the defocus regulator. A holistic TEM dynamical simulator is also under preparation (see http://www.tejadaruiz.net/MBW). Future research will focus on the integration of defocus regulation with other control loops in the microscope (e.g., the beam deflectors).

## Acknowledgments

This work is carried out as part of the Condor project, a project under the supervision of the Embedded Systems Institute (ESI) and with FEI company as the industrial partner. This project is partially supported by the Dutch Ministry of Economic Affairs under the BSIK program. The authors also acknowledge Dr. Sandra Van Aert (EMAT, U. Antwerp) for the fruitful discussions on TEM technology; Dr. Richard Doornbos (ESI) and Dr. Seyno Sluyterman (FEI Company) for their help in the experimental setups; Ir. Stefan Kuiper (DCSC) for his insights in automatic control concepts; and Professors Dirk Van Dyck and Paul M.J. Van den Hof for their help in sharpening the ideas presented here.

## Appendix A. Available auto-tuning methods

Table A1 lists a small selection of auto-tuning methods and some of their properties. For closed-loop control purposes, only those methods capable of measuring (estimating) optical parameters are relevant.

## Appendix B. Estimation of the second-order model parameters

Recall from Section 4 that each identification experiment was composed of two tests. To fit model (6) to the experimental data, the latter was compared, in the minimum square error sense, to the model's ideal response to input signal (7), which is given by [13]

$$\Delta f(t;\theta,\xi,\omega)=\Delta f_{ini}+\Delta f_{step}\left(1-\frac{\lambda_2}{\lambda_2-\lambda_1}(e^{\lambda_1(t-T_{step})}-e^{\lambda_2(t-T_{step})})\right),$$

where $t \geq T_{step}$, $\theta=(T_{step},\Delta f_{ini},\Delta f_{step})$ is the input signal parameter set, $\lambda_1=-\xi\omega+\omega\sqrt{\xi^2-1}$, and $\lambda_2=-\xi\omega-\omega\sqrt{\xi^2-1}$. Note that for every experiment, two estimates of $\theta$, $\hat{\theta}_1$ and $\hat{\theta}_2$ were needed (one per test), while only one estimate of $\xi$ and $\omega$ ($\hat{\xi}$ and $\hat{\omega}$) was needed (the same model should be valid for both tests). $\hat{\theta}_j=(\hat{T}_{step_j},$

**Table A1**
A small selection of available auto-tuning procedures and some of their properties.

| *References* | *Needed images*[a] (*minimum*) | *Image type* | *Measurement principle* | *Tuning/measurement target* |
|---|---|---|---|---|
| Saxton et al. [7] | 3 | BF[b]-TEM | Reach image variance extremal | Beam alignment, defocus, astigmatism |
| Bonet–Zinzindohoue [8] | 3 | BF-TEM | Reach extremal of image descriptor | Beam alignment, defocus, astigmatism |
| Coene–Denteneer [6] | 1 | Diffractogram of Amorphous Mat. | Diffractogram minima fitting | Spherical aberration |
| Koster–de Ruijter [5] | 3 | BF-TEM | Beam-tilt tableau | Beam alignment, defocus, astigmatism |
| Ishizuka [35] | 3 | Diffractogram of Amorphous Mat. | Beam-tilt induced defocus change | Three-fold astigm., coma-free alignment |
| Krivanek [36] | 4 | Diffractogram of Amorphous Mat. | Beam-tilt tableau | Three-fold astigmatism |
| Tanaka et al. [37] | 1 | Amorphous Mat. HAADF[2]-STEM | HAADF model fitting | Defocus, astigmatism |
| Saxton [38] | 8 | Diffractogram of Amorphous Mat. | Diffractogram tableau | Astigmatism, coma |
| Dellby et al. [39] | 3 | Ronchigram of Amorphous Mat. | Local magnification analysis | Multiple optical aberrations |
| Barthel [40] | 1 | Diffractogram of Amorphous Mat. | Database matching | Multiple optical aberrations |
| Sawada et al. [41] | 1 | Ronchigram of Amorphous Mat. | Segment autocorrelation analysis | Aberrations up to fifth order |
| Lupini et al. [42] | 1 | Ronchigram of Amorphous Mat. | Local transfer function fitting | Multiple optical aberrations |

[a] The minimum number of images needed for a measurement may vary based on the type (i.e., order) of the measured aberration, on the number of simultaneously measured aberrations, and on the required measurement precision.

[b] In here, BF stands for "bright field" and HAADF for "high-angular, annular dark field".

$\Delta\hat{f}_{ini_j}, \Delta\hat{f}_{step_j}$), $j=1, 2$, was computed as follows: $\hat{T}_{step_j}$ was taken to be the acquisition time of the last image in test $j$ with a defocus value close to $\Delta f_{ini_j}$ (this image was selected manually). $\Delta\hat{f}_{min_j}$ and $\Delta\hat{f}_{step_j}$ were computed from the defocus values estimated from images (using Thon ring analysis [17]) that were acquired, respectively, before and after the lens transients:

$$\Delta\hat{f}_{min_j} = \sum_{i=-9}^{0} \frac{\Delta\hat{f}_{i_j}}{10}, \quad \Delta\hat{f}_{step_j} = \sum_{i=4}^{13} \frac{\Delta\hat{f}_{i_j}}{10} - \Delta\hat{f}_{min_j},$$

where $\Delta\hat{f}_{i_j}$, $i=0, \pm 1, \pm 2, \ldots$, denotes the defocus value estimated from the image acquired at time $t_{i_j} = \hat{T}_{step_j} + i\Delta T_j$, where $\Delta T_j$ is the inverse of the image rate (see Table 2). Finally, for each experiment, $\hat{\xi}$ and $\hat{\omega}$ were computed as follows:

$$(\hat{\xi},\hat{\omega}) = \arg\min_{\xi,\omega} \left\{ \sum_{i=1}^{10} (\Delta\hat{f}_{i_1} - \Delta f(t_{i_1}; \hat{\theta}_1, \xi, \omega))^2 + (\Delta\hat{f}_{i_2} - \Delta f(t_{i_2}; \hat{\theta}_2, \xi, \omega))^2 \right\}.$$

Note that more than 10 data points can be used to estimate $\hat{\theta}$, $\hat{\xi}$, and $\hat{\omega}$ depending on data availability.

## References


[1] S. Van Aert, A.J. den Dekker, A. van den Bos, D. Van Dyck, High-resolution electron microscopy: from imaging toward measuring, IEEE Transactions on Instrumentation and Measurement 51 (4) (2002) 611–615.

[2] M. Oheim, High-throughput microscopy must re-invent the microscope rather than speed up its functions, British Journal of Pharmacology 152 (1) (2007) 1–4.

[3] V. Starkuviene, R. Pepperkok, The potential of high-content high-throughput microscopy in drug discovery, British Journal of Pharmacology 152 (1) (2007) 62–71.

[4] R.P.G. Collinson, Fly-by-wire flight control, Computing & Control Engineering Journal 10 (4) (1999) 141–152.

[5] A.J. Koster, W.J. de Ruijter, Practical autoalignment of transmission electron microscopes, Ultramicroscopy 40 (2) (1992) 89–107.

[6] W.M.J. Coene, T.J.J. Denteneer, Improved methods for the determination of the spherical aberration coefficient in high-resolution electron microscopy from micrographs of an amorphous object, Ultramicroscopy 38 (3–4) (1991) 225–233.

[7] W.O. Saxton, D.J. Smith, S.J. Erasmus, Procedures for focusing, stigmating and alignment in high-resolution electron-microscopy, Journal of Microscopy 130 (2) (1983) 187–201.

[8] N. Bonnet, P.P. Zinzindohoue, Which image parameter(s) for the automation of the electron-microscope? Journal of Electron Microscopy Technique 11 (3) (1989) 196–201.

[9] K.W. Urban, C. Jia, L. Houben, M. Lentzen, S. Mi, K. Tillmann, Negative spherical aberration ultrahigh-resolution imaging in corrected transmission electron microscopy, Philosophical Transactions. A. Mathematical, Physical and Engineering Science 367 (1903) (2009) 3735–3753.

[10] L.G. Bushnell (Ed.), Special issue on the history of controls, IEEE Control Systems Magazine 16 (3) (1996) 14.

[11] R. Murray, K.J. Åström, S.P. Boyd, R.W. Brockett, G. Stein, Future directions in control in an information-rich world, IEEE Control Systems Magazine 23 (2) (2003) 20–33.

[12] R. Westerhof, A survey of literature on controller scheduling, Report WFW 2000.016.-CTB595-00-2097, Eindhoven University of Technology, 2000.

[13] N.S. Nise, Control Systems Engineering, fourth ed., John Wiley & Sons, 2004.

[14] S. Skogestad, I. Postlethwaite, Multivariable Feedback Control: Analysis and Design, John Wiley & Sons, Inc., New York, NY, 1996.

[15] K. Zhou, J.C. Doyle, K. Glover, Robust and Optimal Control, Prentice Hall, Upper Saddle River, NJ, 1996.

[16] B.A. Brandin, W.M. Wonham, Supervisory control of timed discrete-event systems, IEEE Transactions on Automatic Control 29 (2) (1996) 329–342.

[17] A. Tejada, W. Van Den Broek, S. van der Hoeven, A.J. den Dekker, Towards STEM control: modeling framework and development of a sensor for defocus control, in: Proceedings of the 48th IEEE Conference on Decision and Control, Shanghai, China, 2009, pp. 8310–8315.

[18] T. Södeström, P. Stoica, System Identification, Prentice Hall, Hemel Hempstead, UK, 1989.

[19] L. Ljung, System Identification—Theory for the User, Prentice-Hall, Englewood Cliffs, NJ, 1987.

[20] B. Reed, M. Armstrong, N. Browning, G. Campbell, J. Evans, T. LaGrange, D. Masiel, The evolution of ultrafast electron microscope instrumentation, Microscopy and Microanalysis 15 (04) (2009) 272–281.

[21] P.J. van Bree, C.M.M. van Lierop, P.P.J. van den Bosch, Control-oriented hysteresis models for magnetic electron lenses, IEEE Transactions on Magnetics 45 (11) (2009) 5235–5238.

[22] D. Rijlaarsdam, B. van Loon, P. Nuij, M. Steinbuch, Nonlinearities in industrial motion stages—detection and classification, in: Proceedings of the 2010 American Control Conference, Baltimore, MD, 2010, pp. 6644–6649.

[23] M. De Graef, Introduction to Conventional Transmission Electron Microscopy, Cambridge University Press, Cambridge, 2003.

[24] M. Vulovic, B. Rieger, L. van Vliet, A. Koster, R. Ravelli, A toolkit for the characterization of CCD cameras for transmission electron microscopy, Acta Crystallographica Section D—Biological Crystallography 66 (1) (2010) 97–109.

[25] D.B. Williams, C.B. Carter, Transmission Electron Microscopy, A Textbook for Materials Science, Springer, New York, 2009.

[26] G.Y. Fan, J.M. Cowley, The simulation of high resolution images of amorphous thin films, Ultramicroscopy 21 (87) (1987) 125–130.

[27] O.L. Krivanek, A method for determining the coefficient of spherical aberration from a single electron micrograph, Optik 45 (3) (1976) 97–101.

[28] C. Yang, W. Jiang, D.H. Chen, U. Adiga, E.G. NG, W. Chiu, Estimating contrast transfer function and associated parameters by constrained non-linear optimization, Journal of Microscopy 233 (3) (2009) 301–403.

[29] J. Barthel, A. Thust, Aberration measurement in HRTEM: implementation and diagnostic use of numerical procedures for the highly precise recognition of diffractogram patterns, Ultramicroscopy 111 (1) (2010) 27–46.

[30] A. Tejada, A.J. den Dekker, The role of Poisson's binomial distribution in the analysis of TEM images, Ultramicroscopy, doi:10.1016/j.ultramic.2011.08.010, this issue.

[31] J.T.L. Thong, F. Li, High-speed operation of scanning electron microscope lenses, Scanning 19 (4) (1997) 275–280.

[32] H. Klee, Simulation of Dynamic Systems with MATLAB and Simulink, CRC Press Inc., Boca Raton, FL, 2007.

[33] B. Jayawardhana, H. Logemann, E.P. Ryan, PID control of second-order systems with hysteresis, International Journal of Control 81 (8) (2008) 1331–1342.

[34] G.F. Franklin, J.D. Powell, M.L. Workman, Digital Control of Dynamical Systems, third ed., Addison-Wesley, 1998.

[35] K. Ishizuka, Coma-free alignment of a high-resolution electron microscope with three-fold astigmatism, Ultramicroscopy 55 (4) (1994) 407–418.

[36] O. Krivanek, Three-fold astigmatism in high-resolution transmission electron microscopy, Ultramicroscopy 55 (4) (1994) 419–433.

[37] N. Tanaka, J. Hu, N. Baba, An 'on-line' correction method of defocus and astigmatism in HAADF-STEM, Ultramicroscopy 78 (1–4) (1999) 103–110.

[38] W.O. Saxton, A new way of measuring microscope aberrations, Ultramicroscopy 81 (2) (2000) 41–45.

[39] N. Dellby, O. Krivanek, P. Nellist, P. Batson, A. Lupini, Progress in aberration-corrected scanning transmission electron microscopy, Journal of Electron Microscopy (Tokyo) 50 (3) (2001) 177–185.

[40] J. Barthel, Ultra-precise measurement of optical aberrations for sub-ångström transmission electron microscopy, Ph.D. Thesis, Rheinisch-Westfälischen Technischen Hochschule Aachen, March 2007.

[41] H. Sawada, T. Sannomiya, F. Hosokawa, T. Nakamichi, T. Kaneyama, T. Tomita, Y. Kondo, T. Tanaka, Y. Oshima, Y. Tanishiro, K. Takayanagi, Measurement method of aberration from Ronchigram by autocorrelation function, Ultramicroscopy 108 (11) (2008) 1467–1475.

[42] A.R. Lupini, P. Wang, P.D. Nellist, A.I. Kirkland, S.J. Pennycook, Aberration measurement using the Ronchigram contrast transfer function, Ultramicroscopy 110 (7) (2010) 891–898.